Conformational Study of GPI Anchors: the Common Oligosaccharide GPI Anchor Backbone

Franck Chevalier,[a,b] Javier Lopez-Prados,[a] Serge Perez,[b] Manuel Martín-Lomas,[a] and Pedro M. Nieto*[a]

Keywords: GPI anchor / Conformational analysis/ Molecular flexibility/ Molecular modelling / NMR spectroscopy

The solution three-dimensional structure of pseudopentasaccharide **6**, which constitutes the product from the GPI-PLD cleavage of a GPI anchor, has been studied using a protocol which involves a systematic search of the conformational space around the glycosidic linkages, a thorough molecular dynamics study with explicit water molecules and a full NMR analysis study of intramolecular hydrogen bonding in solution. The results indicate that **6** exists in an extended conformation with a considerable flexibility compatible with a hinge-like conformational motion.

Introduction

The enzymatic cleavage of glycosylphosphatidylinositols (GPIs) to produce inositolphosphoglycans (IPGs) has been proposed as a new pathway of intracellular signal transduction which has been investigated in the case of insulin and a variety of neurotrophic and growth factors.[1] The precise chemical structures of the IPG mediators or the GPI precursors and the nature of the specific enzyme involved in GPI hydrolysis remain to be elucidated. With regard to IPG structure, two main structural groups of IPGs have been proposed on the basis of chemical composition and biological activity data: type A IPGs, which inhibit c-AMP dependent protein kinase (PKA),[2] and type P IPGs, which activate pyruvate dehydrogenase phosphatase (PDHPase).[3] Immunological evidence has suggested that type A IPGs present close structural similarity with the GPI anchors which serve to attach proteins to the outer face of cellular membranes.[4] Concerning the nature of the enzyme involved in GPI cleavage, GPI specific phospholipase C (GPI-PLC) or D (GPI-PLD)[5] could be responsible for the release of IPG second messengers, but a detailed study of the specific structural requirements involved in the regulation of GPI cleavage is still lacking.

We have been engaged in a series of synthetic and structural studies aiming to contribute to the elucidation of the molecular basis of this signaling mechanism.[6] These studies have included the design and the synthesis of IPG-like PKA inhibitors fitting into the ATP binding site of PKA.[6l] To this purpose the three dimensional shape of a variety of possible IPG-like structures were thoroughly studied. Thus, the solid-state structure of *O*-2-ammonio-2-deoxy-α-D-glucopyranosyl-(1–6)-D-*myo*-inositol 1,2-cyclic phosphate (**1**) and the solution structure of **1**, *O*-2-ammonio-2-deoxy-α-D-glucopyranosyl-(1–6)-D-*myo*-inositol-1-phosphate (**2**) and *O*-α-D-mannopyranosyl-(1–4)-*O*-2-ammonio-2-deoxy-α-D-glucopyranosyl-(1–6)-D-*myo*-inositol-1,2-cyclic phosphate (**3**), which constitute the minimum structural motifs to be expected for a GPI-PLC-generated type A IPG, were determined.[6b] Also the solution three dimensional structure of **4**, the molecule to be expected from the GPI-PLC cleavage of a GPI anchor, was studied in detail.[6c] The solution three-dimensional structure of **1** and **2** was determined using NMR spectroscopy[7] and molecular mechanics calculations.[6b] In the case of **3**[6b] and **4**[6c] molecular dynamics simulations in the presence of explicit water were carried out in addition to the NMR analysis. It was concluded that the three-dimensional structure around the *O*-2-ammonio-2-deoxy-α-D-glucopyranosyl-(1–6)-D-*myo*-inositol glycosidic linkage in these zwitterionic species may be described by a major conformer that undergoes torsional oscillations around a global minimum in which the charged ammonium and phosphate groups appear close in space.[6b] The study of **4** also confirmed[8] the existence of the pseudopentasaccharide structure in an extended conformation which undergoes large torsional oscillations around the Man-α-(1–6)-Man linkage and permitted to define the dynamics of this bond by a fast 60:40 equilibrium of *gg*/*gt* rotamers.

With regard to IPG-like structures lacking a phosphate group, which may be generated by the action of a GPI-

[a] Grupo de Carbohidratos, Instituto de Investigaciones Químicas, CSIC,
Isla de la Cartuja, Américo Vespucio 49, 41092 Seville, Spain
Fax: +34-95-446-0565
E-mail: Pedro.Nieto@iiq.csic.es
[b] Centre de Recherches sur les Macromolécules Végétales (CERMAV), CNRS,
B. P. 53, 38941 Grenoble cedex 9, France
Supporting information for this article is available on the WWW under http://www.eurjoc.org or from the author.

 DOI: 10.1002/ejoc.200500171

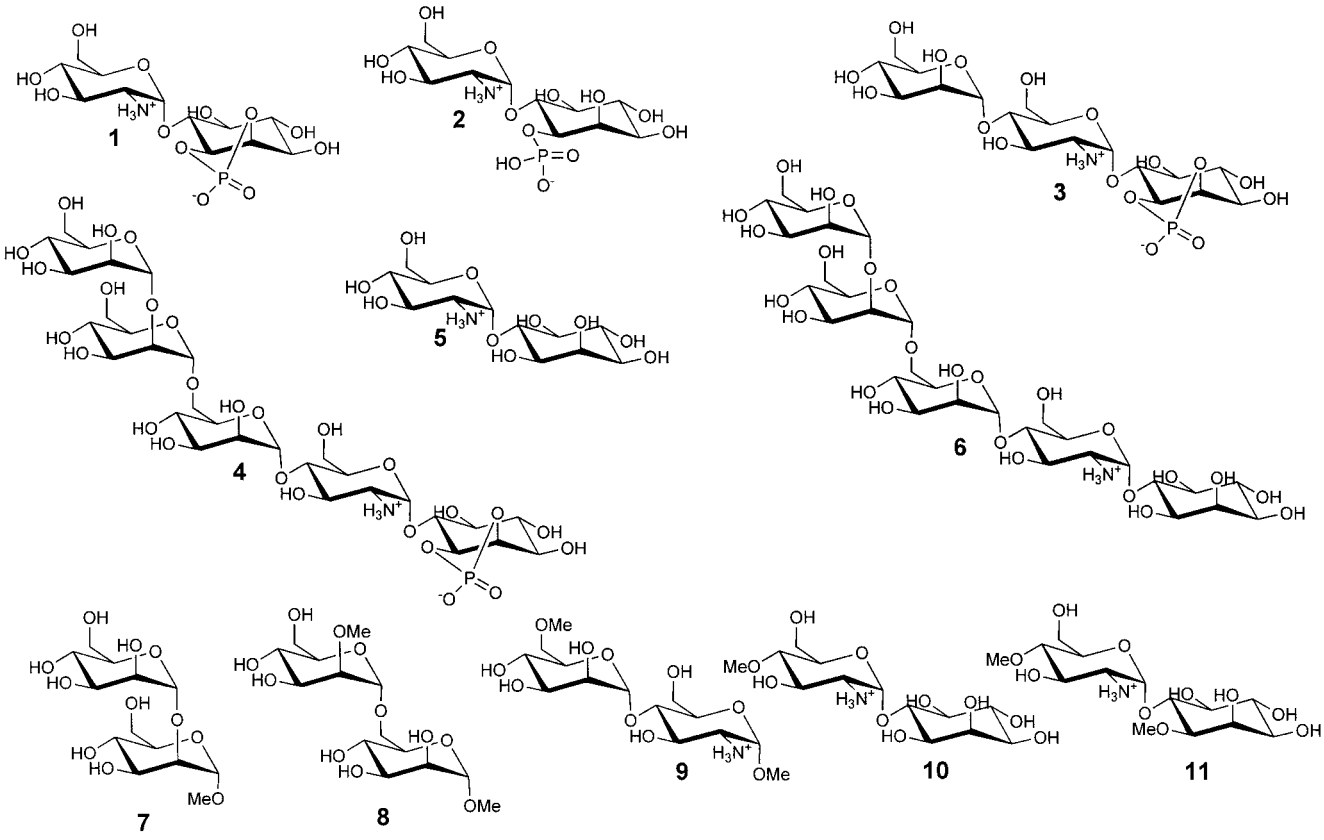

PLD, we have previously reported the solution conformation of *O*-2-amino-2-deoxy-α-D-glucopyranosyl-(1–6)-D-*myo*-inositol (**5**).[6f] In this case the presence of a minor conformer, in addition to the major one observed in the case of **1** and **2**, could be detected. This could be accounted for by considering a higher flexibility of this glycosidic linkage in **5** as a result of the lack of the strong electrostatic interaction present in **1** and **2**. As a part of these studies we now report a complete study of the solution conformation of pseudopentasaccharide **6**, the molecule to be expected from the GPI-PLD cleavage of a GPI anchor. In this case, the study has been based on a combination of NMR spectroscopy and molecular modeling, using both adiabatic maps and molecular dynamics simulations in explicit solvent. In addition, an analysis of intramolecular hydrogen bonding has been performed.

Results and Discussion

The structural study of **6** has been performed using molecular modelling and NMR spectroscopy. First, a systematic conformational analysis of **6** was performed by calculating the Φ,Ψ adiabatic maps for each glycosidic linkage using the MM3 force field. These calculations, which have provided all the favourable structures and their relative stability, have been completed with molecular dynamics simulations, using the GLYCAM force field to gain information on the molecular flexibility and the effect of explicit solvent on the overall structure.

Molecular Modelling

The systematic search of the conformational space around the glycosidic linkages has been performed by constructing Φ,Ψ adiabatic maps for each of the four glycosidic bonds in the linear structure **6** (Man^{V}-α-(1–2)-Man^{IV}; Man^{IV}-α-(1–6)-Man^{III}; Man^{III}-α-(1–4)-$GlcN^{II}$ and $GlcN^{II}$-α-(1–6)-*myo*-Ins^{I}) as isolated glycosidic linkages in the following disaccharide units: α-D-mannopyranosyl-(1–2)-1-*O*-methyl-α-D-mannopyranoside (**7**), 2-*O*-methyl-α-D-mannopyranosyl-(1–6)-1-*O*-methyl-α-D-mannopyranoside (**8**), 6-*O*-methyl-α-D-mannopyranosyl-(1–4)-1-*O*-methyl-(2-amino-2-deoxy)-α-D-glucopyranoside (**9**) and 4-*O*-methyl-(2-amino-2-deoxy)-α-D-(1–6)-1-*O*-methyl-D-*myo*-inositol (**10**). These maps are shown in Figure 1.

The adiabatic map for the Man^{V}-α-(1–2)-Man^{IV} linkage shows two stable minima at Φ = 90°, Ψ = 170° and Φ = 80°, Ψ = 100°, connected through a low-energy pathway, suggesting the coexistence of both wells with fast transitions between them. Similar structures (Φ = 90°, Ψ = 100–170°) have been proposed as stable conformations for the Man-α-(1–2)-Man moiety in complex oligosaccharides or in isolated disaccharides.[9] An additional unstable minimum at Φ = 90°, Ψ = 300°, which corresponds to the stacked conformation found for mannose oligosaccharides,[10] could be also observed (Figure 1).

The adiabatic surface calculated for the Man^{IV}-α-(1–6)-Man^{III} glycosidic bond corresponds with the large flexibility characteristic of the 1–6 glycosidic linkages.[8] Two wide minima were detected at Φ = 80°, Ψ = 190° and Φ = 80°,

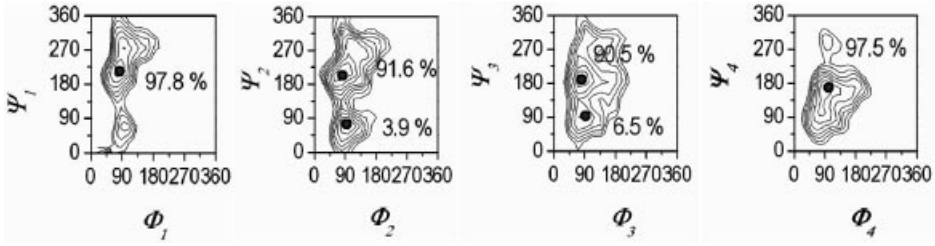

Figure 1. Φ and Ψ adiabatic maps for **7**, **8**, **9** and **10**.

$\Psi = 80°$, defining a large conformationally accessible space covering the region defined by $\Phi = 60–100°$ and $\Psi = 50–310°$.

Two stable minima were found for the Man^{III}-α-(1–4)-GlcN^{II} glycosidic linkage at $\Phi = 90°$, $\Psi = 210°$ and at $\Phi = 100°$, $\Psi = 70°$. The well located around $\Phi = 90°$, $\Psi = 210°$ displayed a complex shape containing two stable subminima differing by only 0.24 kcal/mol of energy corresponding to the *gg* and *gt* rotamers of the hydroxymethyl group of the D-glucosamine unit. The GlcN^{II}-α-(16)-*myo*-Ins^{I} map indicated some flexibility for the corresponding glycosidic linkage as reflected in the wide accessible area observed in the calculated energy surface. The overall energetic landscape for this moiety is comparable to that observed for compound **5**[6f] and not very different for those observed for compounds **1**, **2**[6b] and **4**[6c] using the AMBER force field. However, minor discrepancies related with the evaluation of the relative population of an *anti*-Ψ minimum could be observed. As these discrepancies could be due to the different performance of the force fields used, the influence of the phosphate group was further investigated by constructing the maps for **2** and **5** using the MM3 force field and, in addition, a third model in which the phosphate in **2** was replaced by a non-polar methyl group (**11**) was studied. Not surprisingly, the results indicated (Supporting information; for supporting information see also the footnote on the first page of this article) that the overall shape of the maps was similar in the three models and that the relative stability and weight of the low-energy regions vary as a function of the substituent at position 1 of the *myo*-inositol unit. Thus, the fine details of the conformational preferences of this linkage seem to be modulated by a combination of steric effects and polar interactions.

In summary, the combination of the minimum-energy torsional angles for the glycosidic linkages obtained in this study yielded four low-energy stable structures, as depicted in Figure 2.

The above molecular mechanics study was further completed by performing molecular dynamics (MD) simulations in order to assess the validity of the structures obtained by molecular mechanics and to improve the analysis of the conformational behaviour of pseudopentasaccharide **6** by considering its flexibility features. Several independent starting structures were considered and parallel MD simulations were performed in order to explore a wider conformational space than with a single long simulation.[11] The starting structures were constructed considering the main relative and global minima found in the above adiabatic surface analysis (Figure 1). The hydroxymethyl group ω angles were initially set to the *gt* rotamer except for the D-glucosamine residue for which, according to the previous molecular mechanics study, the *gg* rotamer was also included. Thus, the structures were constructed from the adiabatic map data, four of them (A–D, cf. Figure 2) with the D-glucosamine *gt* rotamer and two more with the D-glucosamine *gg* rotamer (E based on A and F based on C). These six structures were subjected to 2.0 ns MD simulations in explicit water, except for structure B which was subjected to a 4.0 ns MD. The values of the Φ/Ψ dihedral angles along the trajectories showed transitions between several conformations which were essentially similar to those found in the molecular mechanics analysis (Figure 1). This indicates that the inclusion of explicit water in the simulations does not substantially alter the conformation of the most stable structures. In the course of the simulations some interconversions between energy wells were observed indicating that the predicted minima were accessible. Unfortunately, the length of the runs was not long enough as to reach a steady state; therefore it was not possible to quantify the conformer populations in the equilibrium. However, the observed patterns of interconversions suggest that the relative stability of the stable minimum may be different

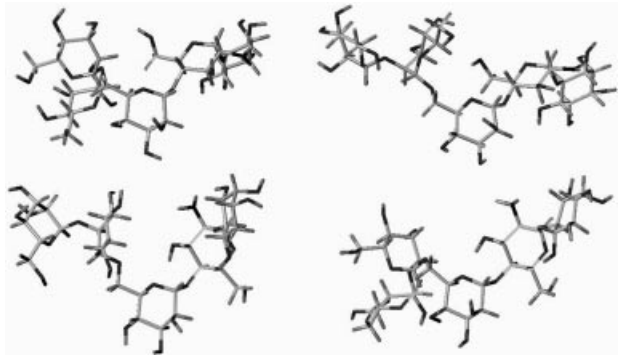

Figure 2. Representation of the four low-energy structures derived from the analysis of adiabatic surfaces for pseudopentasaccharide **6**: in order of stability A (top right), B (top left), C (bottom right), and D (bottom left).

from that estimated from the adiabatic maps. The trajectories of the glycosidic Φ/Ψ dihedral angles indicate that the Man^{V}-α-(1–2)-Man^{IV} linkage fluctuates predominantly around the absolute minimum found in the adiabatic map at $\Phi = 90°$ and $\Psi = 170°$ with transitions towards another region at $\Phi = 80°$ and $\Psi = 120°$. This conformational equilibrium among these previously established conformations,[10–12] is analogous to that described for the L-serine

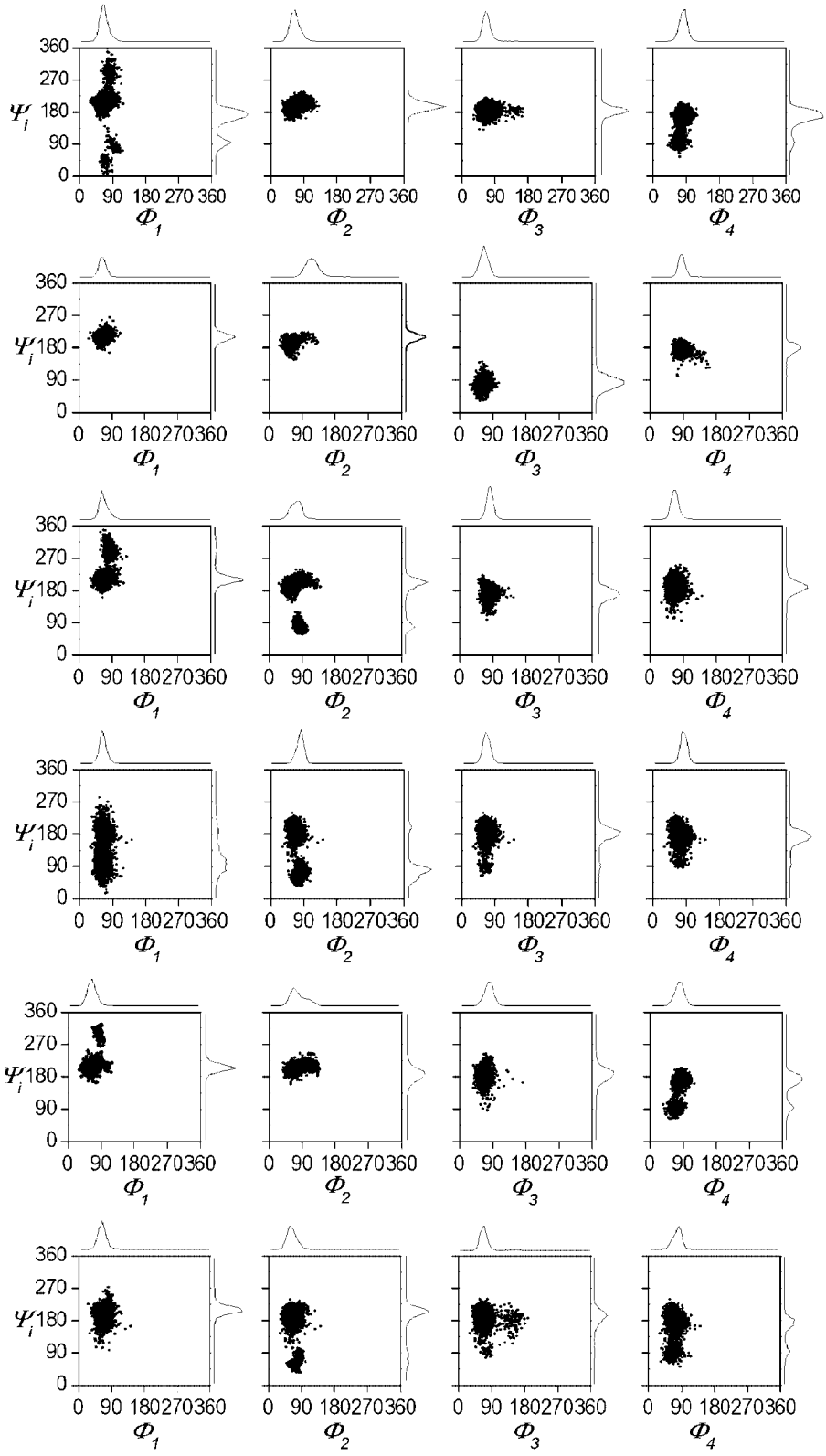

Figure 3. Instant values for the glycosidic Φ/Ψ torsional angles, GlcN^{II}-α-(1–6)-mIns^{I}, Man^{III}-α-(1–4)-GlcN^{II}, Man^{IV}-α-(1–6)-Man^{III}, Man^{V}-α-(1–2)-Man^{IV} (left to right), for the MD runs using A–F (top to bottom) starting structures.

derivative of the disaccharide Man-α-(1–2)-α-D-Man.[14] In agreement with the energy surface analysis, no evidence of stacked conformers at $\Phi = 60°$ and $\Psi = 300°$ were observed in the simulations.

As for the Man^{IV}-α-(1–6)-Man^{III} moiety the MD trajectories confirm, according to the results derived from the adiabatic maps, that this linkage is the most flexible of the pseudopentasaccharide structure. This motif has been extensively modelled as component of oligosaccharides with high mannose content and in most of the cases stable structures around $\Phi = 60°$ and $\Psi = 180°$ have been proposed.[10,12,13] Although, this consensus conformation resulted to be the most stable along the MD runs of **6**, another less-visited structure was observed at $\Phi = 70°$ and $\Psi = 90°$. Several examples of a similar behaviour have been reported as a function of the position of the 1–6 glycosidic linkage in the oligosaccharide chain, this bond being more flexible when located in outer positions.[10,12] Along the MD simulations, the ω angle of the α-(1–6) linkage showed stable trajectories corresponding to *gt* or *gg* rotamers, as reported for the external Man-α-(1–6)-Man moiety of the $Man_9GlcNAc$ oligosaccharide.[10] However, the simulations were not long enough as to reach the steady state and the relative stability of these rotamers could not be accurately evaluated.[15]

The Man^{III}-α-(1–4)-$GlcN^{II}$ linkage trajectories also displayed a fairly high degree of conformational flexibility (Figure 3). The two minima predicted from the energy surface analysis were observed; they remained stable along the duration of the MD simulations. Transitions from the less stable well ($\Phi = 100°$ and $\Psi = 70°$) towards the most stable minimum ($\Phi = 90°$ and $\Psi = 210°$) were clearly observed.

With regard to the $GlcN^{II}$-α-(1–6)-*myo*-Ins^{I} linkage, the most visited structure was also the most stable conformation predicted by the MM study at ($\Phi = 80°$ and $\Psi = 170°$–$240°$). Repeated transitions to a similar structure at $\Psi \approx 300°$ together with less frequent transitions towards the *anti*-Ψ region, at $\Psi \approx 60°$, were detected throughout the molecular dynamic runs. Although, the quantitative analysis of populations of the potential energy surfaces lead us to discard the minimum at $\Psi \approx 60°$, this region corresponds to a clear relative minimum on the energy surface. The minor differences between the MM and MD analysis are purely quantitative, probably due to small differences on the force field but the results of both analyses qualitatively converge.

Figure 4 summarizes these results showing the instantaneous structures for **6** along the six MD simulations. These structures were clustered in six families based on their glycosidic linkage torsional angles. These clusters can be related to the minimum energy structures proposed by energy surface analysis; they depict a gradation of global shapes for **6** ranking from extended to clearly folded conformations. The degree of folding of the structure could be easily described by monitoring the distance between the extremes (*O*-3 of *myo*-Ins^{I} and *O*-4 of Man^{V}). It varies from 20 Å for the extended forms to 12 Å for the folded ones, the extension of the intermediate conformations varying from 15 to 17 Å. During the simulations some transitions between forms belonging to different families were detected in spite. These results fit to a global hinge-like movement as already proposed for **4** based mainly on NMR spectroscopic data,[6c] which in this case is now more adequately described by the MD simulations.

The probability of intramolecular hydrogen-bond formation, which may stabilise a particular conformation of these *myo*-inositol compounds,[16] have also been analysed along the molecular dynamics runs. The following hydroxy groups met the criteria for hydrogen-bond donors: OH3 of Man^{IV}, OH6 and OH3 of $GlcN^{II}$, OH5 and OH1 of *myo*-Ins^{I}. The respective acceptors were: O1 of Man^{V} for OH3 of Man^{IV}; O1 of Man^{III} for OH3 of $GlcN^{II}$; O1 or O5 of Man^{III} for OH6 of $GlcN^{II}$ and O1 of $GlcN^{II}$ alternatively for both OH5 and OH1 of the *myo*-Ins^{I}. Only the pair O1 of Man^{V} and OH3 of Man^{IV} was classified as persistent hydrogen bond through all the six MD runs. The drastic reduction on the *gg*, *gt*, *tg* conformational transitions, from 30 to 9, observed for the $GlcN^{II}$ hydroxymethyl group in comparison with the other units may reflect with the engagement of this group in hydrogen bonding.[12,13]

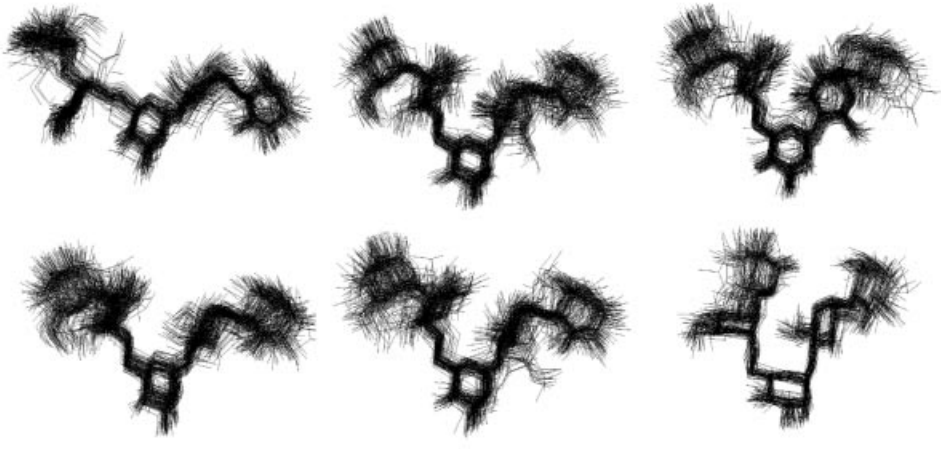

Figure 4. Snapshots saved every 20 ps for the MD simulations clustered by Φ/Ψ torsional angles.

Summarizing, a modelling protocol based on a combination of independent molecular mechanics calculations and molecular dynamics simulations enables an exhaustive exploration of the glycosidic linkages conformational space and an accurate description of the dynamical features of pseudopentasaccharide **6** in the presence of water. In spite of the different force field and conditions, the excellent agreement of the geometries of the stable structures predicted by both methods deserves to be remarked. Only very small quantitative differences related to local details were observed between the two analyses. The combination of these two methods provides simultaneously a suitable graphical description of the global flexibility of the pseudopentasaccharide together with an exhaustive and accurate local definition of the energies and geometries occurring at every glycosidic linkage.

NMR Spectroscopy

The results obtained from the molecular modelling studies were validated using experimental information derived by NMR spectroscopy. The 500 MHz ^{1}H NMR spectrum of **6** was fully interpreted using a combination of COSY, TOCSY, ROESY, NOESY and ^{13}C-HSQC experiments (Supporting information). The sequential assignment was based on the observation of the corresponding inter-residue NOEs and confirmed by the downfield shift of the corresponding carbon resonance. The coupling constant values (Supporting information) proved the expected $^4C_1$ conformation of the monosaccharidic residues. The values of the coupling constants calculated after the stereospecific assignment of the H6 protons were used to calculate the populations of rotamers of the mannose and glucosamine residues,[17] finding a *gg*/*gt*/*tg* ratio of 55:50:0 for Man^{V} and Man^{IV}; 60:40:0 for Man^{III} and 74:13:10 for GlcN^{II}. The inter- and intra-residue NOEs were analyzed from the 2D NOESY spectra using different mixing times ranging from 100 to 1000 ms at 283 K, 298 K and 303 K. The experiments that were recorded at room temperature at 500 MHz showed simultaneously negative and positive weak NOE cross-peaks, indicating that, under these conditions, the $\omega\tau_c$ value of **6** is close to the NOE null point at 1.22. The effect of the temperature on the NOESY experiments established that the origin of this effect is the dependence of the NOE on the molecular tumbling. Moreover, the ROESY spectra showed equivalent positive ROE pattern independently of the temperature thereby confirming the proposed nature of the effect and excluding other possible causes for the changes of intensity and sign of the NOE cross-peaks. The observed dispersion resides on the distribution of effective correlation times which are themselves a function of the global and internal motions. As the global motion should be the same for all the interproton vectors of the same molecule, the differences on effective correlation times must arise from specific contributions due to the local flexibility. The pattern of observed NOEs corresponds to a relatively rigid central region with negative NOE effect and flexible extremes with positive NOE. This experimental observation confirms the MD analysis of the flexibility of **6**, where hinge-like motions around the centre were predicted. Considering the MD model of motion together with rigid residues, the effect of the internal motions should be smaller in the centre of mass of the molecule and it should increase along the backbone towards the extremes were it should be a maximum.

Not all the expected NOE cross-peaks were observed at room temperature; this is due to the low intensity of the peaks close to the null point. However, a maximum number of 25 intra-residue and 7 inter-residue NOE cross peaks were detected under adequate conditions. The significant NMR experimental distances calculated for **6**, and **4**[6b] and for the GPI anchor of the VSG glycoprotein[18] at the equivalent temperature (Table 1) are very similar within experimental error, indicating that all the three oligosaccharides display a common geometry. The distances observed for the inositol end (H6-*myo*-Ins^{I}↔H1-GlcN^{II} and H4-GlcN^{II}↔H1-Man^{III}) are closest for the non-phosphorylated compound **6** than for **4**. This observation suggests an influence of this group on the local structure as it has been determined for compounds **1**, **2** and **3**.[6b] The agreement between the experimental key distances and the calculated values from the adiabatic maps (MM) for **6** indicates the adequacy of the molecular mechanics results about the accessible conformational space of the glycosidic linkages along with their relative flexibility. The MD simulations performed on **1** followed a protocol to explore in the most efficient way the conformational space available by using several starting structures. Due to that, the distances calculated as the $<r^{-6}>$ average over the six runs might not represent a steady state ensemble and, therefore, could not describe accurately the behaviour of **6**.

Finally, the presence of stable intermolecular hydrogen bonds, pointed out by the MD simulations, was investigated by NMR spectroscopy.[7] Such an investigation implies the

Table 1. Significant inter-proton distances calculated from NMR spectroscopic data for **4**,[6b] VSG GPI,[18] and **6**, and calculated by MM for **6**.

	VSG GPI by NMR	**4** by NMR at 283 K	**6** by NMR at 283 K	**6** by NMR at 308 K	**6** by MM
myo-Ins^{I}-H6 GlcN^{II}-H1	2.60	2.36	2.62	2.10	2.28
GlcN^{II}-H4 Man^{III}-H1	2.40	2.23	2.38	3.10	2.38
Man^{III}-H6R Man^{IV}- H1	n. d.	2.67	2.63	3.05	2.66
Man^{III}-H6S Man^{IV}- H1	n. d.	2.20	2.59	2.82	2.37
Man^{IV}-H1 Man^{V}-H3	n. d.	3.03	n. d.		4.50
Man^{IV}-H1 Man^{V}-H5	2.50	2.60	2.50	2.34	2.80
Man^{IV}-H2 Man^{V}-H1	2.30	2.30	2.29	2.21	2.27

detection of the hydroxy protons in H_2O solution using specific NMR experiments in acetone/water solvent mixtures, which requires in general low temperatures and a careful control of the pH.[19] Once the hydroxy resonances are detected, the occurrence of stable hydrogen bonds can be deduced from the changes in chemical shift upon bonding, decrease of the solvent exchange rate, by the line width, the exchange EXSY cross-peaks, or by the temperature coefficient.[20]

By using firstly the mixture acetone/water (15:85) and 1D-NMR and 2D TOCSY experiments (Supporting information), the labile protons of **6** were detected and assigned at 259 K. Unfortunately, the exchange with the solvent was still too fast as to detect NOEs or exchange peaks from the OH signals valid as indicative of hydrogen bonding even using short mixing times. The temperature coefficients were not calculated because the range of detection, between 263 and 259 K, was too small to guarantee reliability. A comparison of the proton chemical shifts between the monomer and the pseudopentasaccharide was performed (Table 2).[19] The protons identified by MD as potential hydrogen-bond donors, with the exception of OH3 of $GlcN^{II}$, are among those that underwent the largest variations: (i) the OH6 of Man^{V} with a downfield shift of 0.09 ppm; (ii) the OH3 of Man^{IV} with a downfield shift of 0.29 ppm; (iii) the OH6 of $GlcN^{II}$ with an upfield shift of 0.74 ppm and OH3 of $GlcN^{II}$ with an upfield shift of 0.15 ppm.

Table 2. Chemical shift differences and temperature coefficients calculated at 500 MHz for hydroxy protons of pseudopentasaccharide **6** at 259 K in acetone/water (85%/15)% and in DMSO/water [1:3 (v/v)].

Hydroxy group		Acetone/water (85%/15%, v/v)	DMSO/water (1:3, v/v)	
		Δδ	Δδ	Δδ/ΔT
Man^{V}	OH2	0.08	0.06	8.13
	OH3	0.06	0.32	9.36
	OH4	0.08	n. d.	n. d.
	OH6	0.09	–0.02	11.15
Man^{IV}	OH3	0.29	0.17	7.16
	OH4	0.09	n. d.	n. d.
	OH6	0.00	n. d.	n. d.
Man^{III}	OH2	0.29	0.06	n. d.
	OH3	0.10	0.106	n. d.
	OH4	0.11	n. d.	n. d.
$GlcN^{II}$	OH3	–0.15	n. d.	n. d.
	OH6	–0.74	–0.95	8.49
myo-Ins^{I}	OH1	0.47	0.108	8.44
	OH2	0.21	0.205	8.00
	OH3	0.15	0.348	7.66
	OH4	0.18	0.158	7.74
	OH5	0.04	0.09	7.84

In order to increase the range of temperatures for the observation of the hydroxy signals, a DMSO/water (25:75, v/v) solvent mixture was used. Under these conditions, the chemical shift variation of the hydroxy resonances with respect to the monomers were similar to those obtained in water/acetone (Table 2). It is known that DMSO as solvent slows down the chemical exchange among hydroxy protons and enhances the formation of H bonds,[21] which could be disrupted by a protic solvent such as water.[22] In fact, when this solvent mixture was used, it was possible to detect the exchangeable protons in a wider range of temperature than with acetone, from 273 to 253 K, making possible to determine some temperature coefficients (Table 2). The temperature coefficients (k), which are known to be dependent on the solvent used,[21] had intermediate values and did not allow to detect definitely those hydroxy groups engaged in a persistent hydrogen bond. However, the lowest k value, corresponding to the less exchangeable hydroxy proton was observed for OH3 of Man^{IV} (k = 7.16), while OH6 of Man^{V}, which is exposed to the solvent and should exchange quickly with the solvent, has the largest value (k = 11.2). Finally, even under the most favourable conditions, it was not possible to detect strongly hydrogen-bonded hydroxy groups by NOE or exchange peaks.

Thus, the exchangeable protons NMR study did not allow us to undoubtedly assess the occurrence of strong hydrogen bonds. However, some correlation between the temperature coefficients and the chemical shift variations with the MD results seems to indicate a relative protection from the exchange with the solvent for some hydroxy groups located in the concave side of the molecule which is the less hydrophilic region of the molecule.

Conclusions

The present study has been focused on pseudopentasaccharide **6** which constitutes the IPG-like structure derived from GPI-PLD hydrolysis of a membrane GPI. Although GPI and IPG structures have already been studied by NMR spectroscopy and molecular modelling, the present study of **6** has allowed a higher level of accurate characterization, in particular by using a protocol which involved a systematic search of the conformational space around the glycosidic linkages, a thorough molecular dynamics study with explicit water molecules and a full NMR analysis including a study of intramolecular hydrogen bonds in aqueous solution.

The low-energy structures have been determined by means of a systematic conformational search of all glycosidic linkages using molecular mechanics. The most stable structures were obtained by relaxing the energy of models as constructed by combining the low-energy conformers at each glycosidic linkage. The most stable of these conformers corresponds to the extended structure imposed by the *syn*-Ψ arrangement of all glycosidic linkages, but other relative minima corresponding to bent structures are also predicted. Subsequent extensive exploration of the conformational space by parallel molecular dynamics simulations yielded families of clustered structures related by conformational transitions. The global shape of these families corresponds to the low-energy structures and varies from extended to markedly folded geometries, the global flexibility arising from the combination of the limited oscillations of all glycosidic linkages. Both, the molecular mechanics calculations (MM3 force field) and the molecular dynamics simulations (GLYCAM-AMBER force field) gave consistent re-

sults that were experimentally validated using NMR spectroscopy. The existence of intramolecular hydrogen bonds, predicted by the calculations, has also been substantiated using NMR spectroscopy by detecting the hydroxy resonances in aqueous solution and observing changes in the chemical shifts and temperature coefficients. The NMR spectroscopic data were not conclusive of the existence of any persistent hydrogen bond; only one of the candidates, OH6 of $GlcN^{II}$, showed experimental data indicative of its implication on a hydrogen bond.

In summary, the analysis of **6** indicates an extended structure with a considerable flexibility compatible with a hinge-like overall motion. As this compound represents the GPI basic carbohydrate moiety, and considering the mechanical role of the GPI anchor as linker between membrane and proteins, this flexibility could be connected to their function as it will control the orientation and free space of the attached protein with respect to the membrane.

Experimental Section

Material: Pseudopentasaccharide **6** was synthesised according to methods which have been essentially described in the literature. A detailed description of this synthesis will be reported elsewhere.[23]

Molecular Modelling: The dihedral angles Φ, Ψ and ω are defined according to IUPAC definition, as O5–C1–O1–$C_{x'}$, C1–O1–$C_{x'}$–$C_{x+1'}$ and O5–C5–C6–O6, respectively, where $C_{x'}$ and $C_{x+1'}$ are the aglyconic atoms. For α-D-Manp-(1–6)-α-D-Manp, Φ is defined as O5–C1–O1–C6′, Ψ as C1–O1–C6′–C5′ and ω as O1–C6′–C5′–OR′, where OR′ is the endocyclic ring oxygen group.

Adiabatic and Probability Maps: The adiabatic maps (Φ,Ψ) for all constituting disaccharides were constructed from the corresponding relaxed energy surfaces calculated by molecular mechanics using MM3(92) force field.[24,25] These adiabatic maps are the two-dimensional projections of a multidimensional hyperspace, where each (Φ,Ψ) point represents all the different orientations of the hydroxy and hydroxymethyl exocyclic groups considered in the relaxed maps. The starting structures where constructed using only the most favourable conformation for each monosaccharide ($^4C_1$ chair for α-D-2-deoxy-2-aminoglucopyranose and α-D-mannopyranose). For each monosaccharide the three staggered orientations for the exocyclic hydroxymethyl groups were considered: *gauche-gauche* (*gg*), *gauche-trans* (*gt*), *trans-gauche* (*tg*) in addition to the two orientations of secondary hydroxy groups, namely *clockwise* (*c*) and *reverse clockwise* (*r*).[26] These considerations lead to the construction of 36 structures for each disaccharide and 12 for the D-*myo*-inositol containing a pseudodisaccharide. From these starting conformers the corresponding relaxed surfaces were obtained by energetic minimization of the 1369 points obtained by the variation of Φ and Ψ angles from 0° to 360° using a 10° grid step. Finally, the adiabatic surfaces were constructed by selecting, for a given (Φ,Ψ) pair, the lowest energy structure among the relaxed maps. Thus, each adiabatic map is composed of 36 relaxed maps involving 49284 energy points with the exception of the ones including D-*myo*-inositol pseudodisaccharides, where 12 maps and 16428 points where used. The Boltzmann probability maps were calculated from all the relaxed maps for each disaccharide. The points with energies larger than 2 kcal/mol from the global energy minimum were disregarded in this calculation. Assuming that the entropy difference among the different conformers in negligible, the probability P of a given (Φ,Ψ) point was calculated by:

$$P_{\Phi,\Psi} = \sum_{i} \frac{\exp(-E_i / RT)}{\sum_{\Phi,\Psi} \exp(E_{i,\Phi,\Psi} / RT)}$$

The inter-protonic distances were calculated as the sixth power averaged distances weighted by its Boltzmann probability along the whole Φ,Ψ space according to:

$$< r^{-6} >_{\Phi,\Psi} = \left[\sum_{\Phi,\Psi,i=1}^{i=n} (P_{\Phi,\Psi,i} r_{\Phi,\Psi,i}^{-6}) \right]^{-1/6}$$

Molecular Dynamics: Molecular dynamic simulations of **6**, both in vacuo and with explicit water, were performed using the AMBER 5 suit of programs[27] and GLYCAM specific force field for carbohydrates.[28] Partial charges have been calculated using the HF/6-31 G* basis set with Gaussian98[29] and RESP method according to the Cornell et al. 1994 force field. The 2.0 ns molecular dynamic runs in explicit water were performed using 2100 TIP3P type water molecules[30] solvating the pseudopentasaccharide using periodic boundary conditions in a rectangular box, of approximately 45 Å × 39 Å × 35 Å. The virtual concentration of the pseudopentasaccharide was 25 mM, in order to compare with an NMR sample concentration. All simulations were carried out in the NPT ensemble, performed at 300 K as described in the literature[31] and at a pressure of 1 bar. The temperature was kept constant using the Berendsen coupling algorithm.[32] The SHAKE[33] algorithm was applied to all bonds involving hydrogen atoms with a tolerance of 0.0005 Å and an integration time step of 2.0 fs was used. Particle Mesh Ewald (PME) method was used to account for long-range electrostatic interactions, and van der Waals interactions were subjected to a 9 Å cut off. A multistep equilibration protocol was used. First, a minimization of the solvent, followed by a short MD run (25 ps) holding on both the pseudopentasaccharide coordinates fixed using a constraint of 500 kcal/mol, an additional minimization was performed allowing only the water molecules to move. The procedure was continued with 5 equilibration cycles composed by a minimization and a sort MD (10 ps) decreasing the constraint applied on the solute (25, 20, 25, 10 and 5 kcal/mol). Finally, an unconstrained MD run of 20 ps was performed in order to reach and stabilize the temperature at 300 K. During this procedure, the cut off for van der Waals interaction was 9 Å, the integration time step 2.0 fs and SHAKE was performed during all MD runs. The analysis of the molecular dynamics simulations data was performed using CARNAL and ANAL modules of the AMBER package.[34] The coordinates of the whole system, density and temperature were calculated and saved every picosecond. The stability of the simulations was checked by a stable behaviour of the Root Mean Square Deviation of the atoms along the trajectories; for density and temperature of the system, see Supporting information. The geometrical criteria for the occurrence of hydrogen bonds were: a distance between hydrogen-bond acceptor and donor shorter than 3.3 Å, and an angle comprised between 120 and 180°. Only pairs fulfilling these geometrical conditions during more than the 20% of the length of each MD run were considered hydrogen-bonded. Molecular surfaces were calculated using SYBYL 6.8.[35] The Connolly solvent accessible surfaces were generated using a radius probe of 1.4 Å, and Poisson–Boltzmann electrostatic potential surfaces were calculated using RESP partial charges for a solvent dielectric constant of 80. Other types of surfaces were obtained according to the software.

NMR: NMR experiments were recorded with a Bruker Avance DRX-500 spectrometer at 283, 298, and 308 K. The pseudopentasaccharide **6** was dissolved in D_2O (500 μL) after several cycles of deuterium exchange, the pH* was adjusted to 6.9 to yield a 7.3 mM sample. 2D spectra were acquired in the phase-sensitive mode using the time-proportional phase incrementation mode:[36] COSY,[37] DQF-COSY,[38] TOCSY,[39] NOESY,[40] ROESY[41] or echo *anti*-echo HSQC.[42] The size of the acquisition data matrix was typically of 2k and 512 points in the *f*2 and *f*1 dimensions for the homonuclear experiments and 1k × 256 for the heteronuclear ones. Processing of the spectra was done with standard Bruker software. A shifted squared sinebell window function was applied to the 2D data matrix before Fourier transformation, and baseline correction was applied. The NOESY spectra were acquired using nine mixing times: 150, 200, 250, 300, 400, 450, 500, 700, and 1000 ms. Coupling constants ^3J(H,H) were calculated from the 2D-DQF-COSY cross peaks using DECO software.[43] NOE-derived inter-proton distances were estimated from the cross-correlation relaxation rates (σ_{NOE}) considering the isolated pair of spin approximation, and an isotropic tumbling of the pseudopentasaccharide, and using as reference distances H1–H2 of glucosamine 2.45 Å and H1–H2 of mannose 2.53 Å. The dipolar relaxation rates were calculated as the initial slope of the NOE growing rate, which were estimated as the first order derivative and at time $t = 0$, $f'(0) = P1P2$ of the curve: normalized NOE volume $f(t) = P1\times[1 - \exp(-P2\times t)]$ determined by fitting the normalized NOE vs. the mixing time.[44] The assignment of $H6_{pro\text{-}R}$ and $H6_{pro\text{-}S}$ has been based on the values of the $^3J_{5,6}$ coupling constants and on the chemical shifts for the H6 protons. According to the observations and the results reported previously,[11,17] a large value is expected for $^3J_{5,6pro\text{-}R}$ and a smaller one for $^3J_{5,6pro\text{-}S}$, and the $H6_{pro\text{-}R}$ signal suffers an upfield shift for the non-reducing residue and a downfield shift for the reducing one. The NMR experiments for the detection of the hydroxy groups were performed with Bruker DRX-600 and DRX-500 spectrometers using a 10.4 mM sample of pseudopentasaccharide dissolved in mixtures of 85% H_2O and 15% [D_6]acetone for the detection experiments and in water and [D_6]DMSO (3:1, v/v) for the measurement of the temperature coefficients. The pH was carefully adjusted to 6.9 prior to the addition of the cosolvent. A 3 mm NMR tube (300 μL) was previously soaked in a 50 mM solution of phosphate buffer (pH = 7) to minimize adsorption of impurities from glassware.[22] Temperature coefficient experiments were recorded at 298, 293, 273, 268, 263, 258, and 253 K. Water suppression was performed by inserting a watergate module[45] previous to the acquisition. Gradient-enhanced or selected versions of TOCSY, ROESY, NOESY experiments were used. ROESY and NOESY spectra were recorded with mixing times of 50, 100, and 200 ms with 1k spectra of 2k data points. TOCSY spectra were recorded using 5, 10, 20, 60, and 100 ms of mixing time with 1k spectra of 2k data points. The composing monosaccharides (α-D-methylmannopyranoside, D-glucosamine and *myo*-inositol) were also studied at the same temperature (259 K) using ^{1}H 1D- and 2D-COSY experiments for the assignment.

Acknowledgments

We thank Prof. Lennart Kenne and Dr. Corine Sandström for their precious help with hydroxy detection technique, Alain Rivet for his support in molecular modelling, and D. Anne Milet for Gaussian access at the LEDSS (http://www-chimie.ujf-grenoble.fr/LEDSS/RESUM/resum.html) and the CECIC at the Institut de Chimie Moléculaire, Grenoble. We would like to thank the European Union for a predoctoral fellowship (TMR programme: Grant HRN-CT-2000-00001/GLYCOTRAIN).

[1] For reviews see: a) D. R. Jones, I. Varela-Nieto, *Int. J. Biochem. Cell. Biol.* **1998**, *30*, 313–316; b) M. C. Field, *Glycobiology* **1997**, *7*, 161–168; c) P. Stralfors, *BioEssays* **1997**, *19*, 327–335.
[2] J. M. Mato, K. L. Kelly, A. Abler, L. Jarret, *J. Biol. Chem.* **1987**, *262*, 2131–2137.
[3] J. Larner, L. C. Huang, C. F. Schwarz, A. S. Oswald, T. Y. Shen, M. Kinter, G. Z. Tang, K. Zeller, *Biochem. Biophys. Res. Commun.* **1988**, *151*, 1416–1426.
[4] a) G. Romero, G. Gómez, L. C. Huang, K. Lilley, L. Lutrell, *Proc. Natl. Acad. Sci. USA* **1990**, *87*, 1476–1480; b) J. Represa, M. A. Avila, C. Miner, F. Giráldez, G. Romero, R. Clemente, J. M. Mato, I. Varela-Nieto, *Proc. Natl. Acad. Sci. USA* **1991**, *88*, 8016–8019; c) J. Represa, M. A. Avila, G. Romero, J. M. Mato, F. Giráldez, I. Varela-Nieto, *Dev. Biol.* **1993**, *159*, 257–265.
[5] D. R. Jones, M. A. Avila, C. Sanz, I. Varela-Nieto, *Biochem. Biophys. Res. Commun.* **1997**, *233*, 432–437.
[6] a) N. Khiar, M. Martín-Lomas, in: *Carbohydrate Mimics. Concepts and Methods* (Ed.: Y. Chapleur), Wiley-Interscience, Weinheim **1998**, pp. 443–462 and references cited therein; b) H. Dietrich, J. F. Espinosa, J. L. Chiara, J. Jiménez-Barbero, Y. León, I. Varela-Nieto, J. M. Mato, F. H. Cano, C. Foces-Foces, M. Martín-Lomas, *Chem. Eur. J.* **1999**, *5*, 320–336; c) M. Martín-Lomas, N. Khiar, S. García, J.-L. Koessler, P. M. Nieto, T. W. Rademacher, *Chem. Eur. J.* **2000**, *6*, 3608–3621; d) M. Martín-Lomas, M. Flores-Mosquera, N. Khiar, *Eur. J. Org. Chem.* **2000**, 1539–1545; e) M. Martín-Lomas, M. Flores-Mosquera, J. L. Chiara, *Eur. J. Org. Chem.* **2000**, 1547–1562; f) M. Martín-Lomas, P. M. Nieto, N. Khiar, S. García, M. Flores-Mosquera, E. Poirot, J. Angulo, J. L. Muñoz, *Tetrahedron: Asymmetry* **2000**, *11*, 37–51; g) M. B. Cid, J. B. Bonilla, S. Dumarcay, F. Alfonso, M. Martín-Lomas, *Eur. J. Org. Chem.* **2002**, 881–888; h) J. B. Bonilla, J.-L. Muñoz-Ponce, P. M. Nieto, M. B. Cid, N. Khiar, M. Martín-Lomas, *Eur. J. Org. Chem.* **2002**, 889–898; i) M. B. Cid, J. B. Bonilla, F. Alfonso, M. Martín-Lomas, *Eur. J. Org. Chem.* **2003**, 3505–3514; j) N.-C. Reichardt, M. Martín-Lomas, *Angew. Chem. Int. Ed.* **2003**, *42*, 4674–4677; k) M. B. Cid, F. Alfonso, M. Martín-Lomas, *Carbohydr. Res.* **2004**, *339*, 2303–2307; l) J. López-Prados, F. Cuevas, N.-C. Reichardt, J.-L. de Paz, E. Q. Morales, M. Martín-Lomas, *Org. Biomol. Chem.* **2005**, *3*, 764–786.
[7] J. Jimenez-Barbero, T. Peters (Eds.), *NMR Spectroscopy of Glycoconjugates*, Wiley-VCH, Weinheim, **2003**.
[8] S. W. Homans, C. J. Edge, M. A. J. Ferguson, R. A. Dwek, T. W. Rademacher, *Biochemistry* **1989**, *28*, 2881–2887.
[9] V. S. R. Rao, P. K. Qasba, P. V. Balaji, R. Chandrasekaran, in *Conformation of carbohydrates*, Harwood Academic Publishers, Amsterdam, **1998.**
[10] R. J. Woods, A. Pathiaseril, M. R. Wormald, C. J. Edge, R. A. Dwek, *Eur. J. Biochem.* **1998**, *256* 372–386.
[11] B. A. Spronk, A. Rivera-Sagredo, J. P. Kammerling, J. F. G. Vliegenthart, *Carbohydr. Res.* **1995**, *273*, 11–26.
[12] P. K. Qasba, P. V. Balaji, V. S. Rao, *Glycobiology* **1994**, *4*, 805–815.
[13] P. V. Balaji, P. K. Qasba, V. S. Rao, *Glycobiology* **1994**, *4*, 497–515.
[14] K. Lycknert, A. Helander, S. Oscarsson, L. Kenne, G. Widmalm, *Carbohydr. Res.* **2004**, *339*, 1331–1338.
[15] N. K. Kirschner, R. J. Woods, *Proc. Natl. Acad. Sci. USA* **2001**, *98*, 10541–10545.
[16] M. Felemez, B. Spiess, *J. Am. Chem. Soc.* **2003**, *125*, 7768–7769.
[17] R. H. Marchessault, S. Pérez, *Biopolymers* **1979**, *18*, 2369–2374; Y. Nishida, H. Hori, H. Ohrui, H. Meguro, *J. Carbohydr. Chem.* **1988**, *7*, 239–250; P. C. Manor, W. Saenger, D. B. Davis, K. Jankowski, A. Rabazenko, *Biochim. Biophys. Acta* **1974**,

340, 472–483; C. Altona, C. A. G. Haasnoot, *Org. Magn. Reson.* **1980**, *13*, 417–429.
[18] S. W. Homans, M. A. Ferguson, R. A. Dwek, T. W. Rademacher, R. Anand, A. F. Williams, *Nature* **1988**, *333*, 269–272.
[19] C. Sandström, H. Baumann, L. Kenne, *J. Chem. Soc. Perkin Trans. 2* **1998**, 2385–2394.
[20] M. Dobson, L. Y. Lian, C. Redfield, K. D. Topping, *J. Magn. Res.* **1986**, *69*, 201–209.
[21] H. C. Siebert, S. André, F. G. Vliegenthart, H. J. Gabius, M. J. Minch, *J. Biomol. NMR* **2003**, *25*, 197–215.
[22] B. Adams, L. Lerner, *J. Am. Chem. Soc.* **1992**, *114*, 4827–4829.
[23] López Prados Javier, *Inositolfosfoglicanos: Síntesis, Estructuras y Actividad Biológica*, Th. D, Chimie, Universidad de Sevilla, **2004**, p. 310 .
[24] N. L. Allinger, Y. H. Yuh, J. H. Lii, *J. Am. Chem. Soc.* **1989**, *111*, 8551–8566.
[25] N. L. Allinger, M. Rahman, J. H. Lii, *J. Am. Chem. Soc.* **1990**, *112*, 8293–8307.
[26] C.-W. von der Lieth, T. Kozár, W. E. Jull, *J. Mol. Struct (Theochem.)* **1997**, *395–396*, 224–225.
[27] D. A. Case, D. A. Pearlman, J. W. Caldwell, T. E. Cheatham III, W. S. Ross, C. L. Simmerling, T. A. Darden, K. M. Merz, R. V. Stanton, A. L. Cheng, J. J. Vincent, M. Crowley, D. M. Ferguson, R. J. Radmer, G. L. Seibel, U. C. Singh, P. K. Weiner, P. A. Kollman, *AMBER 5*, University of California, San Francisco, **1997.**
[28] R. J. Woods, R. A. Dwek, C. J. Edge, B. Fraser-Reid, *J. Phys. Chem.* **1995**, *99*, 3832–3846.
[29] M. J. Frisch, G. W. Trucks, H. B. Schlegel, G. E. Scuseria, M. A. Robb, J. R. Cheeseman, V. G. Zakrzewski, J. A. Montgomery, R. E. Stratmann, J. C. Burant, S. Dapprich, J. M. Millam, A. D. Daniels, K. N. Kudin, M. C. Strain, O. Farkas, J. Tomasi, V. Barone, M. Cossi, R. Cammi, B. Mennucci, C. Pomelli, C. Adamo, S. Clifford, J. Ochterski, G. A. Petersson, P. Y. Ayala, Q. Cui, K. Morokuma, D. K. Malick, A. D. Rabuck, K. Raghavachari, J. B. Foresman, J. Cioslowski, J. V. Ortiz, A. G. Baboul, B. B. Stefanov, G. Liu, A. Liashenko, P. Piskorz, I. Komaromi, R. Gomperts, R. L. Martin, D. J. Fox, T. Keith, M. A. Al-Laham, C. Y. Peng, A. Nanayakkara, C. Gonzalez, M. Challacombe, P. M. W. Gill, B. G. Johnson, W. Chen, M. W. Wong, J. L. Andres, M. Head-Gordon, E. S. Replogle, J. A. Pople, *Gaussian98*, Gaussian, Inc., Pittsburgh PA, **1998.**
[30] W. L. Jorgensen, J. Chandrasekhar, J. D. Madura, R. W. Impey, M. L. Klein, *J. Chem. Phys.* **1983**, *79*, 926–935.
[31] T. E. Cheatham III, J. L. Miller, T. Fox, T. A. Darden, P. A. Kollman, *J. Am. Chem. Soc.* **1995**, *117*, 4193–4194; D. J. Tobias, *Curr. Opin. Struct. Biol.* **2001**, *11*, 253–261.
[32] H. J. C. Berendsen, J. P. M. Postma, W. van Gunsteren, A. DiNola, J. R. Haak, *J. Chem. Phys.* **1984**, *81*, 3684–3690.
[33] P. Ryckaert, G. Ciccoti, H. J. C. Berendsen, *J. Comput. Phys.* **1977**, *79*, 926–935.
[34] D. A. Pearlman, D. A. Case, J. W. Caldwell, W. S. Ross, T. E. III Cheatham, S. DeBolt, D. Ferguson, G. Seibel, P. Kollman, *Comp. Phys. Commun.* **1995**, *91*, 1–41.
[35] SYBYL 6.8: Tripos Inc., 1699 South Harley Rd., St Louis, Missouri 63144, USA.
[36] D. Marion, K. Wüthrich, *Biochem. Biophys. Res. Commun.* **1983**, *113*, 967–974.
[37] W. P. Aue, E. Bartholdi, R. R. Ernst, *J. Chem. Phys.* **1976**, *64*, 2229–2246.
[38] A. L. Davis, E. D. Lane, J. Keeler, D. Moskau, J. Lohman, *J. Magn. Reson.* **1991**, *94*, 637–644.
[39] A. Bax, D. G. Davis, *J. Magn. Reson.* **1985**, *65*, 355–360.
[40] A. Kumar, R. R. Ernst, K. Wüthrich, *Biochem. Biophys. Res. Commun.* **1980**, *95*, 1–6.
[41] A. Bothner-By, R. L. Stephens, J. M. Lee, C. D. Warren, R. W. Jeanloz, *J. Am. Chem. Soc.* **1984**, *106*, 811–813.
[42] A. Bax, A. Aszalos, Z. Dinya, K. Sudo, *J. Am. Chem. Soc.* **1986**, *108*, 8056–8063.
[43] D. Jeannerat, G. Bodenhausen, *J. Magn. Reson.* **1999**, *141*, 133–140.
[44] H. Maaheimo, P. Kosma, L. Brade, H. Brade, T. Peters, *Biochemistry* **2000**, *39*, 12778–12788.
[45] M. Piotto, V. Saudek, V. Sklenar, *J. Biomol. NMR* **1992**, *2*, 661–666; V. Sklenar, M. Piotto, R. Leppik, V. Saudek, *J. Magn. Reson., Ser. A***1993**, *102*, 241–245.

Received: March 7, 2005
Published Online: July 1, 2005

